

Cronfa - Swansea University Open Access Repository

This is an author produced version of a paper published in :
Movement Ecology

Cronfa URL for this paper:
<http://cronfa.swan.ac.uk/Record/cronfa21955>

Paper:

Bidder, O., Walker, J., Jones, M., Holton, M., Urge, P., Scantlebury, M., Marks, N., Magowan, E., Maguire, I. & Wilson, R. (2015). Step by step: reconstruction of terrestrial animal movement paths by dead-reckoning. *Movement Ecology*, 3(23)
<http://dx.doi.org/10.1186/s40462-015-0055-4>

This article is brought to you by Swansea University. Any person downloading material is agreeing to abide by the terms of the repository licence. Authors are personally responsible for adhering to publisher restrictions or conditions. When uploading content they are required to comply with their publisher agreement and the SHERPA RoMEO database to judge whether or not it is copyright safe to add this version of the paper to this repository.
<http://www.swansea.ac.uk/iss/researchsupport/cronfa-support/>



METHODOLOGY ARTICLE

Open Access



Step by step: reconstruction of terrestrial animal movement paths by dead-reckoning

O. R. Bidder^{1*}, J. S. Walker², M. W. Jones², M. D. Holton³, P. Urge⁴, D. M. Scantlebury⁵, N. J. Marks⁵, E. A. Magowan⁵, I. E. Maguire⁵ and R. P. Wilson⁶

Abstract

Background: Research on wild animal ecology is increasingly employing GPS telemetry in order to determine animal movement. However, GPS systems record position intermittently, providing no information on latent position or track tortuosity. High frequency GPS have high power requirements, which necessitates large batteries (often effectively precluding their use on small animals) or reduced deployment duration. Dead-reckoning is an alternative approach which has the potential to ‘fill in the gaps’ between less resolute forms of telemetry without incurring the power costs. However, although this method has been used in aquatic environments, no explicit demonstration of terrestrial dead-reckoning has been presented.

Results: We perform a simple validation experiment to assess the rate of error accumulation in terrestrial dead-reckoning. In addition, examples of successful implementation of dead-reckoning are given using data from the domestic dog *Canis lupus*, horse *Equus ferus*, cow *Bos taurus* and wild badger *Meles meles*.

Conclusions: This study documents how terrestrial dead-reckoning can be undertaken, describing derivation of heading from tri-axial accelerometer and tri-axial magnetometer data, correction for hard and soft iron distortions on the magnetometer output, and presenting a novel correction procedure to marry dead-reckoned paths to ground-truthed positions. This study is the first explicit demonstration of terrestrial dead-reckoning, which provides a workable method of deriving the paths of animals on a step-by-step scale. The wider implications of this method for the understanding of animal movement ecology are discussed.

Keywords: Step length, dead reckoning, animal movement, GPS, terrestrial

Background

Animal movement interests animal biologists because, *inter alia*, it determines the success of individuals in obtaining resources, avoiding predation, maximising fitness and managing energetic profitability [1–3]. The success of individuals modulates populations and drives evolution and the diversity of life [4]. There are also numerous practical benefits to understanding animal movement, such as predicting the impact of land use changes, control of invasive and pest species, conservation of endangered species and foreseeing the spread of zoonotic diseases [5–8].

Obtaining the required information on animal movements is far from trivial, however, as many species

operate in environments that preclude them from being observed (e.g. [9, 10]). Many biotelemetry methods deal with this [11] because they obviate the need for visual contact between researcher and study animal. The two methods most frequently applied in terrestrial environments for obtaining animal location data are VHF and GPS telemetry [12, 13]. Both however, have their limitations [14]; VHF is an established method, but requires significant field effort to implement [15] while GPS telemetry is considered to be ‘accurate’ [16] but prone to bias according to the environment [17, 18], particularly with regard to vegetation [19] and landscape topography [20]. In addition, the high current drain of GPS systems necessitate large batteries when recording at high sampling rates, which limits use on smaller species [21–23], or restricts researchers to deployments of shorter duration [24]. Analysis of data obtained by both methods assumes straight line travel between temporally infrequent

* Correspondence: o.r.bidder@gmail.com

¹Institut für Terrestrische und Aquatische Wildtierforschung, Stiftung Tierärztliche Hochschule, Hannover, Werfstr. 6, 25761 Büsum, Germany
Full list of author information is available at the end of the article

positions [25] even though much animal movement is known to be highly tortuous [26]. Clearly, there is a need for fine-scale animal movement data in both space and time so that animal movement models can better reflect the true nature of animal movement (c.f. [27]).

In fact, the only biotelemetric method purported to produce fine scale (i.e. >1 Hz) terrestrial animal movement data is dead-reckoning [28–30] which may resolve movement so finely that it can even be used to infer behaviour [31]. Dead-reckoning calculates the travel vector for a given time interval using information on heading, speed and change in the vertical axis [32]. Once this is achieved, the three dimensional movement path can be reconstructed by integrating the vectors in sequence [33–35]. Because data are recorded by sensors on board an archival logger, its efficacy is unaffected by the permissiveness of the environment [17, 18] which is important for obtaining accurate, unbiased data [36, 37]. In addition, archival loggers require considerably less power than GPS systems. Typically, a GPS running at 1 Hz may require between 30 and 50 mA of current, where as a modern iteration of the daily diary recording tri-axial acceleration and magnetometer data at 40 Hz requires only 5–10 mA of current (Holton, *pers. comm.*)

Dead-reckoning has been employed for tracking aquatic species [30, 33, 35, 38–40] but is yet to be used for species that utilise terrestrial locomotion. This is partly because of the difficulty for determining the speed of terrestrial animals [41], a process which is simpler underwater where mechanical methods can be used due to the density and viscosity of water [42–50]. However, an ability to estimate speed reliably for land animals should, in fact, make terrestrial dead-reckoning more straightforward than for aquatic or volant species [38] because terrestrial movement is not subject to drift due to air flow [51] or ocean currents [33]. Thus, the primary difficulty for terrestrial dead-reckoning may simply be the measurement of speed, and, were this to be provided, that this approach should provide a means to determine latent positions of animals between less frequent location data obtain by other means of telemetry [38].

Recently though, Bidder et al. [52] have shown that dynamic acceleration, as measured by animal borne inertial sensors, provides a means to estimate speed by proxy. Although the relationship between speed and dynamic acceleration can be perturbed by variations in substrate and incline [53], potential cumulative errors such as these [31, 38] could be corrected by periodic ground-truthing by a secondary means of telemetry. Indeed, this remains the most workable theoretical solution for terrestrial dead-reckoning, with the additional benefit that the use of accelerometers also enables behavioural analysis [54–56]. However, the terrestrial dead-reckoning method and the procedure for

correcting tracks to verified positions has yet to be illustrated explicitly.

The present study details how terrestrial dead reckoning can be achieved using a novel correction method that couples accelerometer and magnetometer data to periodic ground-truths, obtained by a secondary means such as GPS telemetry.

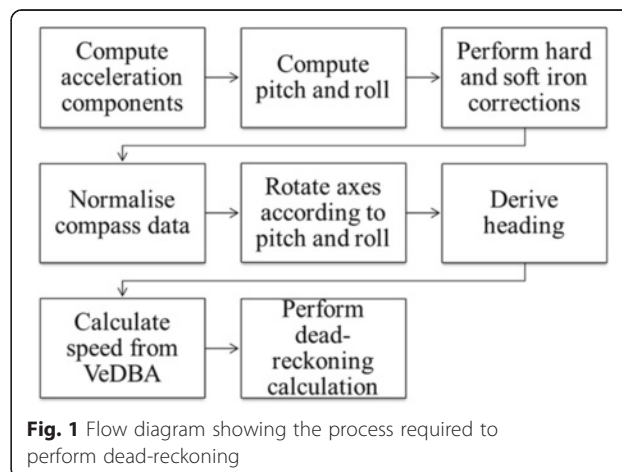
The dead-reckoning procedure for terrestrial animals

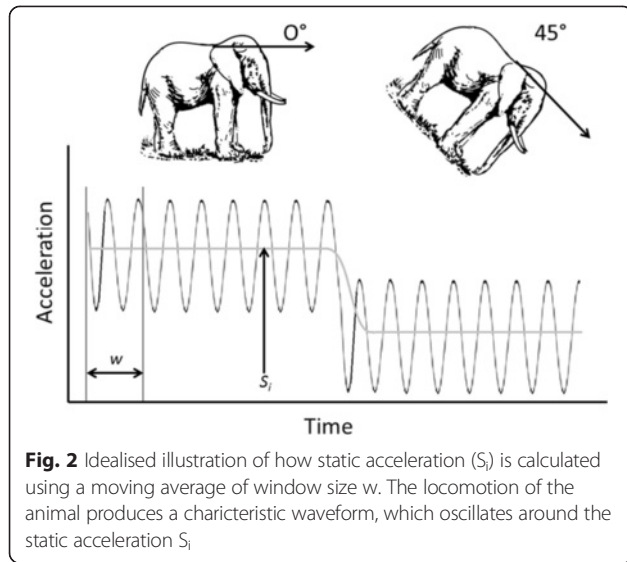
There are a number of stages required to obtain animal travel paths using dead-reckoning (Fig. 1), which require concurrent data from an animal-attached tag containing accelerometers and magnetometers with tri-axial orthogonal sensors recording at infra-second rates (e.g. typically >10 Hz). The stages are treated sequentially in detail below with brief discussion on potential system errors before the approach is trialled on animals to demonstrate performance.

Computing acceleration components

The ‘static’ acceleration [44, 57, 58] is required in order to undertake the necessary pitch and roll calculations for computing compass heading when the device orientation is not level, as is often the case when a tag is mounted on an animal. The static acceleration is that acceleration component due to the pull of gravity and amounts to $1g$ or 9.81 ms^{-2} of acceleration and can be approximated using the method detailed in Shepard et al. [57], using a moving average (see Fig. 2).

The static acceleration for any sample, S_b , given window size w may be computed using the equation given in Fang et al. [59];





$$S_i = \frac{1}{w} \sum_{j=i-\frac{w}{2}}^{i+\frac{w}{2}} S_j$$

The dynamic acceleration (DA_i) can be calculated by subtracting the static acceleration from the raw acceleration recorded by the accelerometer on each of the orthogonally placed axes (x , y & z). These values are then used to calculate VeDBA as described in Qasem et al. [60];

$$VeDBA = \sqrt{(DA_x^2 + DA_y^2 + DA_z^2)}$$

This metric is used as a proxy for speed [53], below, while the static acceleration values are used to help calculate the attitude or pitch and roll of the device. Note that VeDBA values are the instantaneous measurements of dynamic acceleration for any given sample.

Computing pitch and roll from accelerometers

Roll and pitch are calculated as rotations in the sway and heave (or surge) axes, respectively. For clarity, a tri-axial accelerometer records acceleration in the heave, surge and sway axes, corresponding to the dorso-ventral, anterior-posterior and lateral axes of the quadrupedal animal respectively [56]. If the static acceleration of heave, surge and sway are denoted by S_x , S_y and S_z respectively, then pitch and roll can be calculated as (modified from [34]);

$$Roll (\gamma) = \left(atan2(S_x, \sqrt{S_y \cdot S_y + S_z \cdot S_z}) \cdot \frac{180}{\pi} \right)$$

$$Pitch (\beta) = \left(atan2(S_y, \sqrt{S_x \cdot S_x + S_z \cdot S_z}) \cdot \frac{180}{\pi} \right)$$

This calculation normally provides pitch and roll in radians, so the presence of $180/\pi$ provides the result in degrees. The relationship between static acceleration and pitch and roll, is shown in Fig. 3.

Note that *atan2* is a function in computer programming, and is available in Excel, Matlab etc. and calculates the angle between the two coordinates given as arguments (separated by “,”). In standard mathematical formula *atan2* may be expressed as;

$$atan2(y, x) = 2 \arctan \frac{y}{\sqrt{x^2 + y^2} + x}$$

This proposed method calculates pitch and roll based on derivation of static acceleration using low-pass filtering based on a running mean, and is therefore prone to inaccuracies when animal movement is highly variable or sudden [61–64]. However, attitude is often measured using combined accelerometers and gyroscopes [59, 65–67] and certainly gyroscopes calculate attitude more accurately than accelerometers alone [62–64]. The question is whether this makes a real difference in dead-reckoning studies. Certainly, the limited difference in derived attitudes from accelerometers *versus* gyroscopes in wild animal studies [62–64] would imply not, especially since accelerometers alone reliably estimate attitude during periods of steady locomotory activity [59]. In addition, gyroscopes must record at very high sampling rates (>100 Hz), and have substantive power and memory requirements [63, 64] which precludes their use on many free-living animals with realistic package sizes and deployment periods [63, 64]. Indeed, it has been claimed that such inertial reference systems have weight, power requirement and costs that are tenfold those of simple accelerometer systems [68]. Other methods of deriving static acceleration from accelerometers without the need for gyroscopes exist, such as using a combination of Fast-Fourier transformation and low-pass finite impulse response filters [59, 69], or various other low-pass filters and approaches [44, 58, 70, 71]. We used the running mean method because it was already required to calculate the metric for dynamic acceleration, VeDBA [60] and because it has been demonstrably successful. Importantly though, the calculated static acceleration is only obtained to inform the orientation calculations, and the correction method for dead-reckoned tracks (see below) should filter any minor differences generated by using different static acceleration values in this stage of analysis.

Hard and Soft iron corrections for magnetometers

The earth’s magnetic field can be distorted by the presence of ferrous materials or sources of magnetism near the magnetometer and this can result in errors in heading derivation due to the magnetometer’s susceptibility to

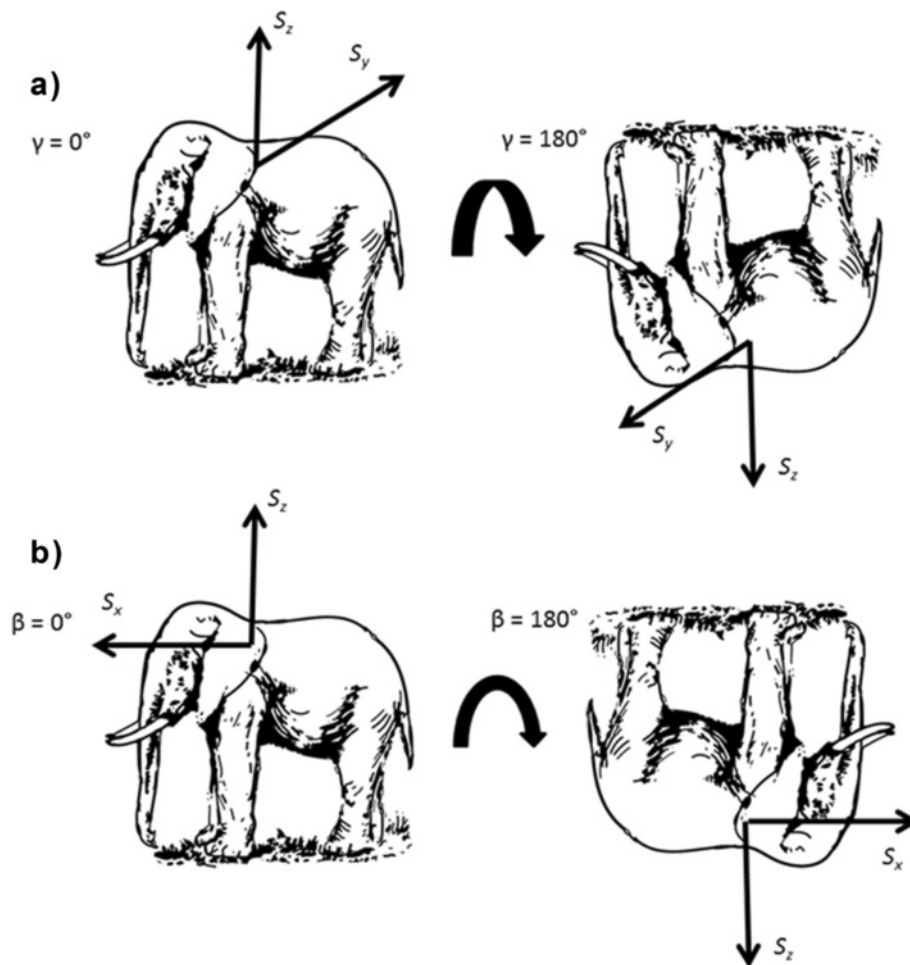


Fig. 3 Illustration of how changes in body orientation, i.e. **a** Roll (γ), **b** Pitch (β), produce changes in static acceleration. S_x represents the Heave axis (dorso-ventral), S_y represents the Surge axis (anterior-posterior), and S_z represents the Sway axis (lateral)

magnetic distortions [72]. Few papers in the biological literature for dead-reckoning give explicit consideration to magnetic deviation in this manner [29–31, 33, 38], despite there being considerable discussion of its impacts within the engineering literature [73–76]. There are two primary sources of error in heading calculation from digital magnetometers; soft iron and hard iron magnetic distortions [77]. In the absence of magnetic distortions and after normalising the compass data for each axis, rotating the magnetometer through all possible orientations should produce a sphere when the data are plotted in a 3-dimensional scatterplot. This is because the magnetic field detected on each axis is the trigonometric product of the vector angle (i.e. heading) between them [78].

Soft iron distortions occur when ferrous material around the sensors (e.g. casing, screws, panels etc.), although not magnetic themselves (i.e. magnetically ‘soft’), alter the magnetic field around the device [68] causing the magnetic field to flow preferentially through them [79]. When a device containing tri-axial magnetometers is rotated under

the influence of consistent soft iron distortions, the resultant data plotted in an X, Y, Z tri-axial magnetic field intensity plot (Fig. 4) are no longer a sphere but an ellipsoid, as the magnetic field observed by the sensors is dependent on the device’s orientation. These can be corrected by using an ellipsoid correction factor on the data before heading calculation provided that the position of the source of the soft iron distortion remains static relative to the movement of the magnetometer [80].

‘Hard’ iron effects are caused by ferrous materials that have permanent magnetism, and thus their own magnetic field [81] and so add a constant magnetic field component that shifts the position of the centre of the sensor output. Correction applies a factor that returns the calibration to an origin of 0,0,0 [82] (Fig. 5).

To calibrate the device so that correction can be undertaken against both hard and soft iron distortions, the tag should be rotated through 360° whilst held level and then rolled 90° and rotated again. This process essentially allows each axis of the magnetometer to obtain

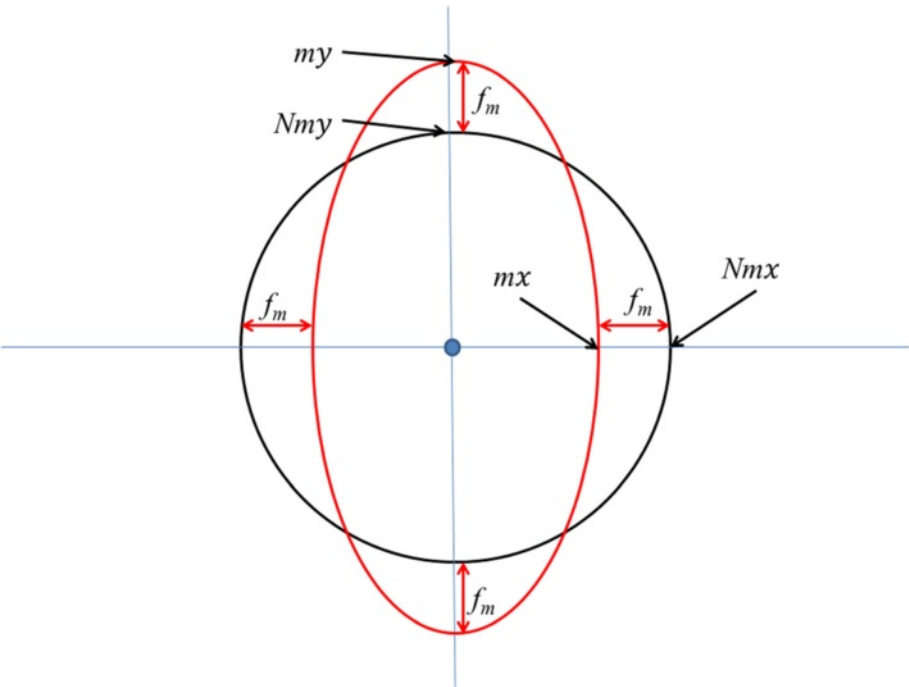


Fig. 4 Visualisation of magnetometer data where distortions in the magnetic field due to soft iron sources near to the sensors may change the expected outputs on the various axes (two of three shown for simplicity). This can be corrected by appropriate normalising procedure (see text)

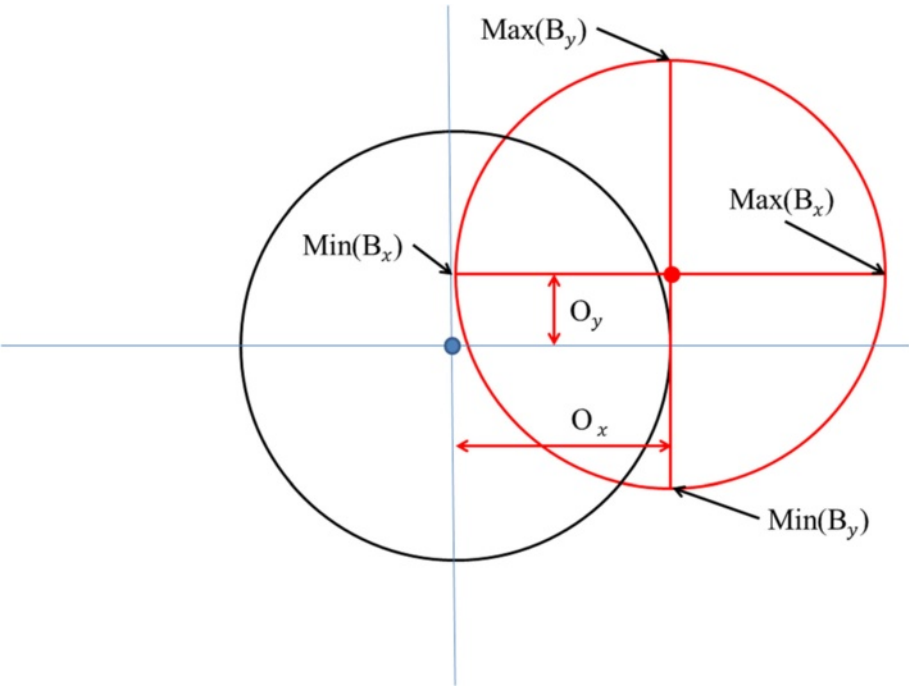


Fig. 5 Visualisation of displacement correction for the magnetometer output in two axes. The red circle represents data for a 360° rotation from two magnetometer axes that are subject to displacement from the true point of origin (black circle) by hard iron distortion

values for the headings of North, East, South and West, denoted as B_x , B_y and B_z . As described in Merkel & Säll [83], for each axis, a minimum and maximum value are obtained, which is then used to calculate the offset produced by hard and soft iron distortions, denoted by O according to;

$$O_x = \frac{\max(B_x) + \min(B_x)}{2}$$

$$O_y = \frac{\max(B_y) + \min(B_y)}{2}$$

$$O_z = \frac{\max(B_z) + \min(B_z)}{2}$$

This offset is then used to correct the output of the magnetometer to give the true magnetism experienced by the sensor on each axis, given as m via;

$$m_x^h = B_x - O_x$$

$$m_y^h = B_y - O_y$$

$$m_z^h = B_z - O_z$$

Normalizing compass data

The compass data can be normalised using a normalising factor f_m [83];

$$f_m = \sqrt{m_x^2 + m_y^2 + m_z^2}$$

This factor is then applied to the outputs of each axis to normalise the magnetometer vector to unit length (Fig. 4) according to;

$$Nm_x = \frac{m_x}{f_m}$$

$$Nm_y = \frac{m_y}{f_m}$$

$$Nm_z = \frac{m_z}{f_m}$$

Rotating axes according to pitch and roll

During device deployment the tag is unlikely to be kept level. This is problematic for the derivation of heading because tilting the device alters the output of the magnetometer due to magnetic declination and inclination angles. Thus, pitch and roll values must be used to calculate what the magnetometer outputs were for the device to be orientated level, denoted by RNm_x , RNm_y and RNm_z ;

$$RNm_i = Nm_i \cdot R_x(\gamma) \cdot R_y(\beta)$$

The rotation matrices (modified from [34]) for pitch and roll, given as $R_y(\beta)$ and $R_x(\gamma)$ respectively are expressed by;

$$R_x(\gamma) = \begin{bmatrix} 1 & 0 & 0 \\ 0 & \cos\gamma & -\sin\gamma \\ 0 & \sin\gamma & \cos\gamma \end{bmatrix}$$

$$R_y(\beta) = \begin{bmatrix} \cos\beta & 0 & \sin\beta \\ 0 & 1 & 0 \\ -\sin\beta & 0 & \cos\beta \end{bmatrix}$$

Derivation of heading

The heading (H) in degrees may be calculated simply (see [84]) via;

$$H = (\text{atan2}(RNm_y, -RNm_x)) \cdot \frac{180}{\pi}$$

Calculation of speed from VeDBA

VeDBA (see above for calculation) is a good (linear) proxy for speed [52, 53] and can be incorporated together with speed (s) via;

$$s = (VeDBA \cdot m) + c$$

where m is the constant of proportionality and c is a constant. During the dead-reckoning process (see below), the value for m can be changed iteratively until dead-reckoned paths and ground truth positions accord. In turn, speed (s) can be used to calculate distance, d , according to the time period length, t , as;

$$d = s \cdot t$$

Dead-reckoning calculation

To overcome Cartesian grid errors on a 3D Earth, it is necessary to determine a speed coefficient, q , using;

$$q = \frac{d}{R}$$

where d is the distance for that time period and R is the radius of the earth (6.371×10^6 m). Latitude and Longitude at time T_i can then be calculated via (sourced from Chris Veness, at <http://www.movable-type.co.uk/scripts/latlong.html>);

$$Lat_i = \text{asin}(\sin Lat_0 \cdot \cos q + \cos Lat_0 \cdot \sin q \cdot \cos H)$$

$$Lon_i = Lon_0 + \text{atan2}(\sin H \cdot \sin q \cdot \cos Lat_0, (\cos q - \sin Lat_0 \cdot \sin Lat_i))$$

Verification of calculated paths

In order to evaluate the accuracy of the calculated paths, synchronous ground-truthing data must be obtained. This

can be achieved through the concomitant use of a secondary means of telemetry such as VHF or GPS. We used GPS, which produces a sequence of Latitude and Longitude values. When GPS and DD are perfectly synchronized, and assuming that the GPS estimates are perfect (but see later), the error in dead-reckoned (D_R) position can be calculated by measuring the distance from a synchronous position obtained from the GPS via (sourced from Chris Veness, at <http://www.movable-type.co.uk/scripts/latlong.html>);

$$Err = \text{acos}(\sin Lat_{DR} \cdot \sin Lat_{GPS} + \cos Lat_{DR} \cdot \cos Lat_{GPS} \cdot \cos(Lon_{GPS} - Lon_{DR})) \cdot 6371$$

where the distance between the two coordinates is given in km. If the coordinates do not accord, the dead-reckoned track can be corrected according to the following procedure; For any time period, the distance between consecutive GPS positions is first calculated. This distance is then divided by the corresponding distance for the same time period calculated by dead-reckoning, providing a correction factor by which dead-reckoning over- or underestimates speed. Subsequently, all speed values (s) for this time period can be multiplied by the correction factor (Fig. 6).

Non-accordance of the two tracks after this is indicative of a heading error, most likely due to the long axis of the tag imperfectly representing the longitudinal axis of the animal. To correct for this, the heading between

the two ground-truthed positions that start and finish the relevant time period is calculated, as is the heading between the start and end positions of the dead-reckoned track. Then, in a manner similar to the correction of speed, the heading for the ground-truthed positions is divided by the heading for the dead-reckoned track to provide the heading correction factor (Fig. 7). This factor is applied to the heading data used in all intermediate dead-reckoning calculations and the dead-reckoned track then recalculated. This procedure of correcting distance and heading continues iteratively until dead-reckoned tracks and ground-truthed positions align.

Results and Discussion

Validation of terrestrial dead-reckoning

In order to validate the dead-reckoning technique we performed a simple experiment at Swansea University, UK. A human participant was equipped with a Samsung Galaxy S5 set to record GPS position every second and Accelerometer and Magnetometer data at 30 Hz. In addition, the participant's position was logged simultaneously using a video camera. Geo-referenced points were obtained by performing a perspective transformation to acquire a top-down view. We manually labelled the position of the participant on each frame of the video, and then transformed the points using known reference positions to latitudinal and longitudinal coordinates. The participant walked a grid pattern within a 40 m by 20 m

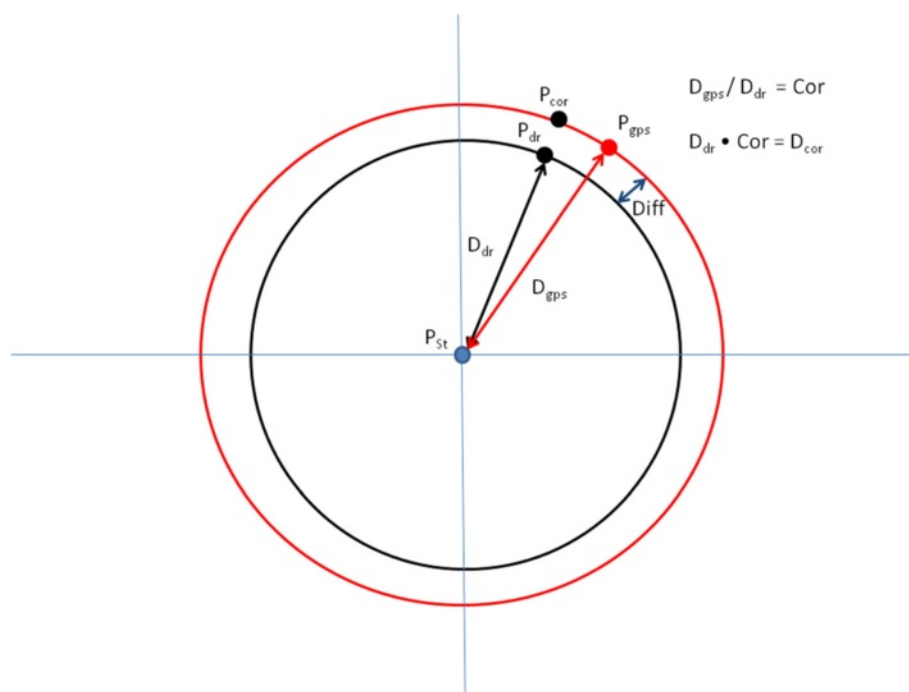


Fig. 6 Illustration of how the distance correction factor is calculated. The correction factor is then applied to all distance calculations so that dead-reckoned and ground-truthed positions accord

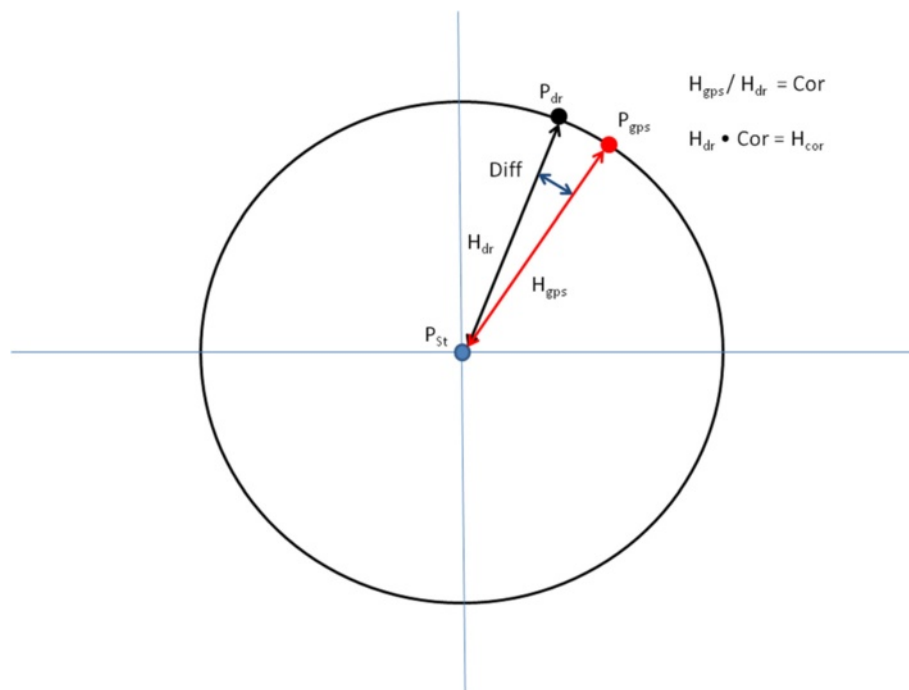


Fig. 7 When distances between two time-synchronized positions derived from both GPS and dead-reckoned are equal but there is displacement between dead-reckoned and GPS-derived positions, a heading error is likely to have occurred but can be corrected (see text)

area on a grass playing field, in front of the camera's field of view. The GPS data obtained was not sufficiently accurate in this instance to be used for ground-truthing the dead-reckoned track (see Fig. 8 panel b). The video positions were sub-sampled down to a position every 1, 2, 5, 10, 15 and 20 s and the dead-reckoning procedure was performed using each of these data sets for ground-truthing. The distance between the dead-reckoned positions during the latent periods (i.e. the periods between ground-truth correction) and the concordant video-derived positions (the complete,

continuous data without sub sampling) was measured and termed the Distance Error. Figure 8 shows a comparison of the tracks dependent on the frequency of ground-truthing. GPS alone did not accurately reproduce the true pattern of movement at this scale. Figure 9 shows the mean Distance Error over the entire experiment at each of the ground-truthing frequencies. As expected, mean Distance Error increased with longer ground-truth intervals. Using a linear regression, we estimate the error accumulation rate to be 0.194 m per second between ground-truth corrections. At this

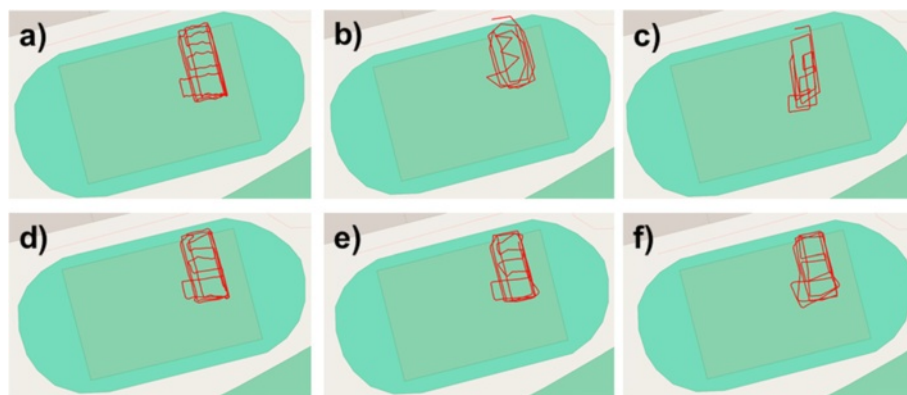
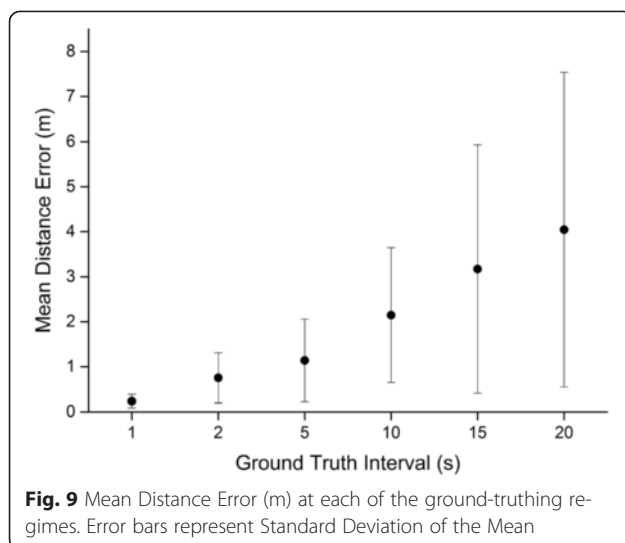


Fig. 8 2D paths of the human participant as determined by **a** Video Recording, **b** GPS, **c** Dead-Reckoning without correction, **d** Dead-Reckoning with correction every 2 s, **e** Dead-Reckoning with correction every 5 s, **f** Dead-Reckoning with correction every 10 s



stage, this figure is merely advisory as the error accumulation of terrestrial dead-reckoning is likely to be highly variable according to animal behaviour, surface type and track tortuosity [38, 53]. Further controlled trials are required to explore this issue. A video of this validation trial, comparing the track calculation according to different ground-truthing frequencies, is available in the supplementary information (see Additional File 1).

Example studies on animals

The viability of the dead-reckoning procedure will be dependent on a large number of particularities (such as the terrain and the quality and frequency of the GPS fixes etc.) associated with the study animal in question. Thus, we present example results of dead-reckoning systems, deployed largely on domestic animals so as to be able to derive errors more readily, to give a general idea of the suitability of this procedure to determine terrestrial animal movements.

'Daily Diary' accelerometer loggers (wildbyte-technologies, Swansea, UK) and 'i-gotU' GPS data loggers (Mobile Action, Taipei City, Taiwan) were used to record both location and movement in a domestic dog (*Canis lupus familiaris*), horse (*Equus ferus caballus*), cow (*Bos Taurus*) and a badger (*Meles meles*) in deployment periods that lasted up to approximately 24 h. Loggers were attached using a leather neck collar to the badger and dog, to the saddle pad of the horse and by a surcingle-belt to the cow. Daily diaries recorded at 40Hz. GPS loggers recorded every 5 s for horse and dogs, 20s for cattle and every 60 min for badgers. Daily diaries weighed 28.0 g and had dimensions 46 × 19 × 39 mm. GPS loggers weighed 21.2 g and had dimensions 13 × 43 × 27 mm. The battery longevity for both the accelerometers and the GPS loggers was approximately 10 days.

Dead-reckoning versus GPS

Dead-reckoning- and GPS-derived positions are fundamentally different but give superficially similar results (Fig. 10). GPS-derived positional data show excellent spatial coherence at scales over 10 m and are independent of time. Dead-reckoned tracks replicate the major features shown by GPS-derived tracks but, when they have no ground-truthed points along them, are uncoupled from the environment and generally show decreasing coherence with respect to themselves over time (Fig. 10). Nevertheless, over small time and scale intervals, dead-reckoned data show features in movement that are often lost in GPS-derived positions. For example, during data acquisition used for Fig. 8, the horse was directed to move in tight circles, which are much better resolved than the GPS data.

GPS-enabled dead-reckoning

The value of using GPS to correct for inaccuracies in dead-reckoned trajectories can be illustrated using GPS-enabled DDs [38] on domestic dogs *Canis lupus familiaris* and horses. Here, we provided conditions where the dogs could move 'freely', as they accompanied their owners, while the horse movement was directed by a rider. In these cases, there was variable discord between GPS positions and dead-reckoned positions for both the dogs and the horse (Table 1). However, calculation of animal travel paths, determining speed according to VeDBA without any form of correction, unsurprisingly, produced appreciable error (Mean = 732 ± 322 m). Once corrections for distance and heading were applied, average distance between GPS and dead-reckoned positions was negligible though (Mean 0.29 ± 0.2 m).

In addition, after correction, the total distance apparently travelled by the animals differed according to whether it was calculated by dead-reckoning or GPS, with dead-reckoned tracks being consistently higher (Table 2) and mean differences between measures of total distance for GPS and dead-reckoning being 0.702 ± 0.465 km. This highlights the effect of enhanced tortuosity displayed by dead-reckoned paths, even when the GPS-derived positions are being recorded at 0.2 Hz.

The difference in poorly, versus highly, defined tracks derived from just GPS and GPS-enabled dead-reckoned trajectories was most apparent in the dogs (Table 2), presumably because, due to their smaller size and active behaviour, dogs were much more likely to deviate from the course defined by the GPS trajectory within any 5 s period of time (Fig. 11). The dead-reckoned track highlights the high degree of tortuosity in the tracks (Fig. 11) but also explains why there was appreciable variation in the correction factors required to tie in the derived speed and heading for dead-reckoned tracks with the GPS positions over time (Fig. 12).

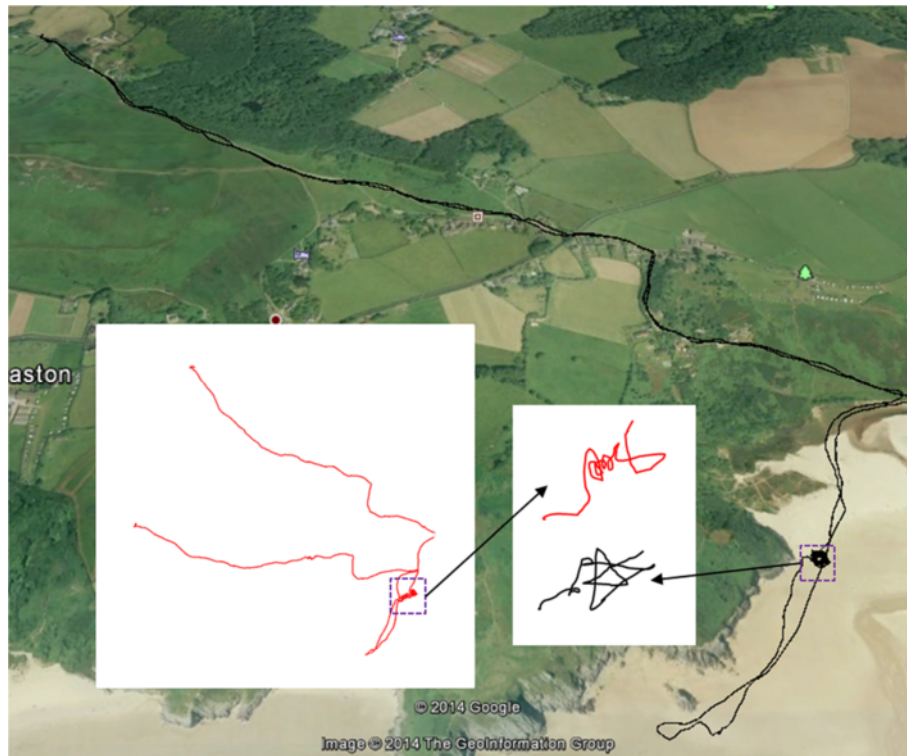


Fig. 10 The movements of a rider-directed horse *Equus ferus caballus*, starting and ending in the *top left corner*, as elucidated by GPS (at 1 Hz - *black track*) and dead-reckoning (at 20 Hz) without any ground-truthed points (*red track*). Note that the dead-reckoned trace has no scale since the distance moved is derived from the speed and this is assumed to be linearly related to VeDBA, with a nominal relationship until ground-truthed (see text). The two dashed squares show a period when the horse was directed to move in tight circles. For scale, the total track length according to the GPS (*black track*) was 10.127 km

In particular, although there was relatively little variation in the speed correction factor over time, the heading correction was, at times, radically different from that initially computed using the acceleration- and magnetometry-derived data (Fig. 12). The cause for this is due, in part to the high frequency of GPS fixes, the

Table 1 Details for accordance between GPS and dead-reckoned positions prior to and post correction procedure for data derived from animals using DDs recording tri-axial acceleration and tri-axial magnetic field strength, with 12-bit resolution, at a sampling frequency of 20 Hz with GPS loggers (iGotU GT-120, Mobile Action Technology) recording at 0.2 Hz. Devices (61 g) were collar-mounted in the dogs, and placed on the saddle pad above the withers in the horse

Subject	Mean Error before correction (m)	Mean Error after correction (m)
Dog 1	591	0.13
Dog 2	653	0.11
Dog 3	480	0.53
Horse	1204	0.39
Mean	731.0	0.29
St. Dev	322.5	0.20

error in those fixes and the speed of the animal. Another possible source of errors may be associated with the estimation of static acceleration (used in the orientation correction of magnetometer data) via smoothing of the data. Further studies should be able to assess this by using more than one method to estimate static acceleration and monitoring if heading estimations differ.

The effect of the errors in the GPS positions on dead-reckoned tracks and the correction factors required to tie these in with GPS positions is likely to increase with increasing GPS sampling frequency because, even though GPS positional estimates are relatively small (of the order of a few metres [18–20, 85]), these become relatively larger as the scale over which movement is considered decreases (Fig. 13).

This highlights why temporally finely resolved GPS positional estimates require such radical heading corrections in headings derived using dead-reckoning. In slow-moving animals such as cows (Fig. 13), GPS fixes can be calculated as being several metres in front of the true position and several metres behind in an animal that is moving slowly in one direction. In such a case, corrected dead-reckoned tracks will, at times, have to use a heading that is the exact opposite of that derived using the magnetometry

Table 2 Summary of track length estimations according to GPS telemetry and dead-reckoning for data presented in Table 1. The tortuosity was calculated as average change in heading between measurements (at 40 Hz)

Subject	GPS Length (km)	Dead Reckoning Length (km)	Difference (km)	Tortuosity (°)
Dog 1	5.507	6.410	0.902	6.38
Dog 2	2.075	2.492	0.418	6.16
Dog 3	3.040	4.296	1.256	11.52
Horse	10.127	10.360	0.233	4.38

data. This problem will presumably diminish as GPS fixes become less frequent and as the speed of the animal increases.

All this emphasises the value of dead-reckoning *per se*, in helping define very fine animal movements (Fig. 14), where such definition may even help identify animal behaviours although such data may not be in perfect spatial placement. Otherwise, dead-reckoning is clearly useful for filling in likely trajectories for animals where positional information via GPS is only gained infrequently although the errors will require much more work to formalise. However, this work points to appreciable problems that will need to be resolved when GPS-based positional information is acquired at high frequencies and dead-reckoning

is to be used to derive a trajectory. One approach is to filter GPS point accuracy according to the number of satellites used to derive the positional fix, or similar metrics such as minimum distance or motion sensor threshold [86]. However, even this will never give perfect spatial resolution. A better way forward may be to combine such metrics with an error circle and consider the extent to which the dead-reckoned path may pass through it.

Potential and pitfalls in ground-truthed terrestrial dead-reckoning

This exploratory work suggests that dead-reckoning is a viable means to track terrestrial animal movements on a fine scale. One notable advantage of terrestrial, compared



Fig. 11 Movement path of a domestic dog. The purple track displays the GPS data (at 0.2 Hz) while the green shows the dead-reckoned path (at 40 Hz). For scale, the total track length according to the GPS was 3.040 km. Note the additional track tortuosity of the dead-reckoned track

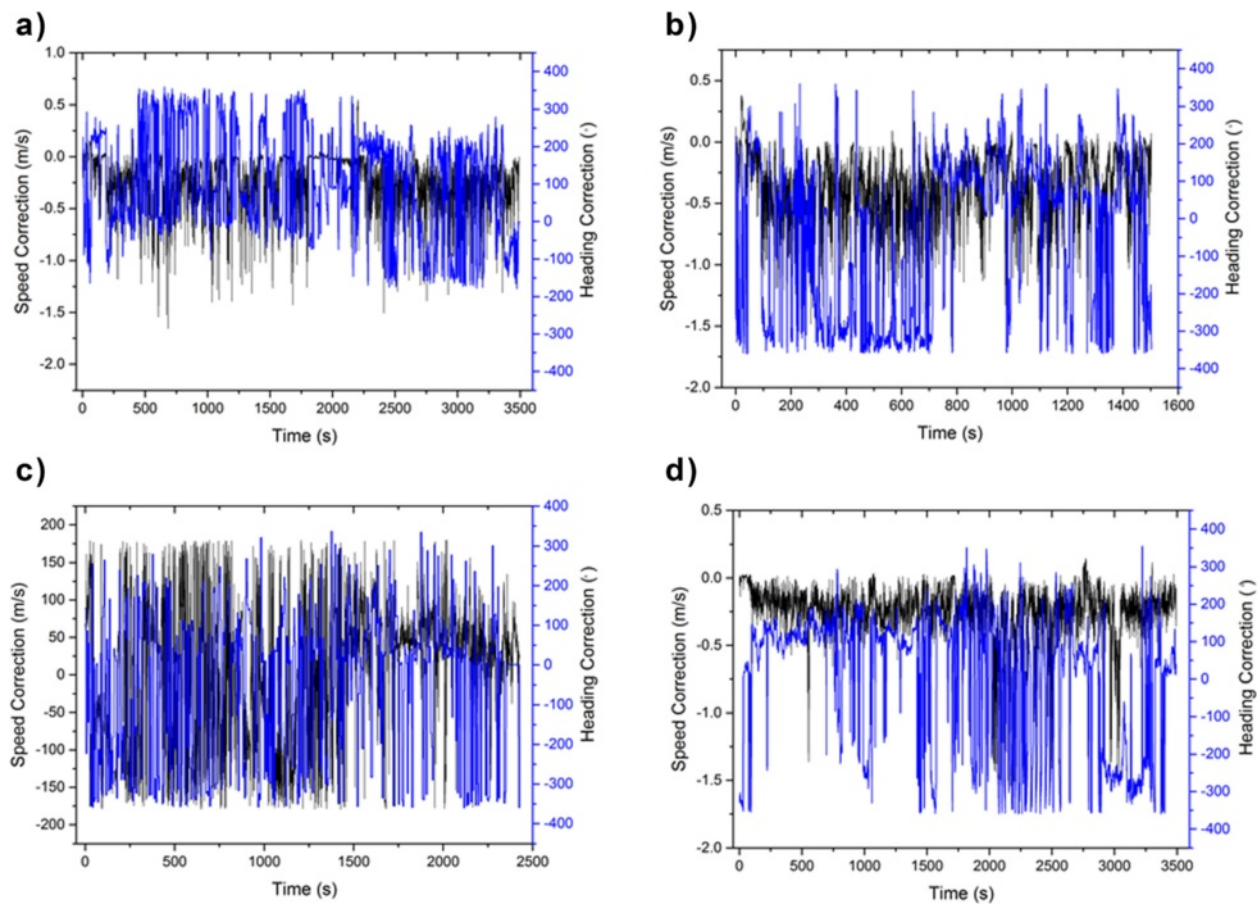


Fig. 12 Changes in speed and heading correction factors necessary to tie dead-reckoned tracks into those acquired by GPS during deployment of a GPS-enabled DD on a) dog 1, b) dog 2, c) dog 3 and d) a horse. Note that the speed correction value changes relatively little but the heading estimates sometimes varied considerably

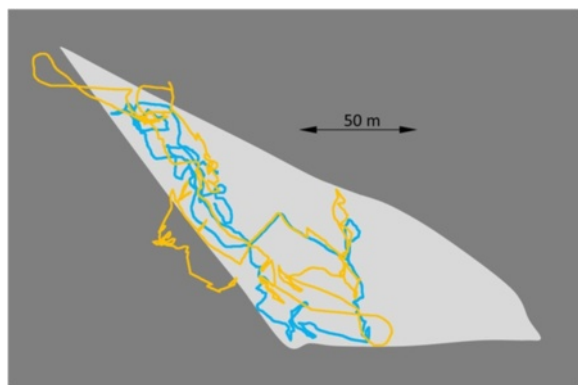


Fig. 13 GPS-enabled dead-reckoned tracks (DD sampling rate 40 Hz, GPS sampling rate 0.1 Hz) from a domestic cow *Bos taurus* in an enclosed field (light grey area) over 2 h. The yellow track shows the calculated trajectory using all GPS points (at 20 s intervals) while the blue track shows the calculated trajectory omitting all unrealistic GPS points (based on speed and estimates outside the peripheral fence). Note that various elements of the GPS, such as the Kahlmann filter, may give highly credible loops within the track that do not correspond to the real trajectory of the animal (cf. yellow lines outside the field periphery)

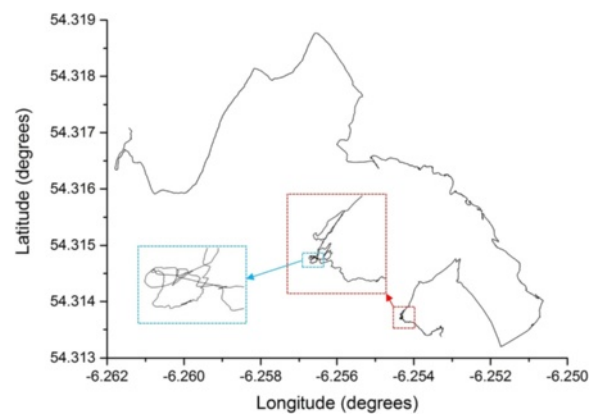


Fig. 14 GPS-corrected (30 min intervals) dead-reckoned (40 Hz) track of a wild badger *Meles meles* over 200 mins during which time the animal was calculated to have moved to a distance of 670 m from its sett. The boxes show zoomed sections of the track to illustrate the effective maintenance of resolution over even short time intervals

to fluid-based dead-reckoning, is that there is no drift due to horizontal vectors such as wind or currents [38]. However, dead-reckoned data must be periodically ground-truthed because system errors, such as imperfect tag orientation on the animal and terrain effects [52, 53], cause the track to become uncoupled from the environment. The appropriate frequency and quality of such ground-truthed points is complex. GPS loggers used on wild animals typically record at fix at periods ranging over seconds [87–89], hours [90, 91], days [92] or even months [93] and have errors that depend on the permissiveness of the environment [18–20, 85] so a clear next stage in this work is to derive a rule book for maximizing the value of both GPS and dead-reckoned data according to the questions being asked. In environments in which accurate GPS locations are not possible (e.g. under dense canopy cover [17, 20, 94–98]) ground-truthing may be more reliably achieved using Radio Frequency Identification (RFID) stations or camera traps at known locations.

Implications of dead-reckoned tracks for understanding movement ecology

While the advantages of GPS-derived data are clear, those of dead-reckoned data have received less attention, perhaps because of the limited number of users. Importantly though, dead-reckoned data show relative movement with very fine resolution, with better coherence of these data the closer they are in time to each other. With the advent of novel open-source analysis software (see [99], in this volume), dead-reckoning may also be implemented with little computational acumen or programming skill. Thus, we expect researchers to be able to use movement defined by dead-reckoned tracks over seconds to be able to resolve behaviours, examining 2- or 3-d space use as a template in the same manner as accelerometry data [56].

Currently, the majority of studies of animal movement are based on infrequent positional fixes obtained via transmission telemetry, calculating distance by assuming straight line travel between fixes [100]. The assumption of such straight line paths ignores sub-fix tortuosity in animal paths [101] and leads to obvious underestimations of animal travel distance, both theoretically (Fig. 2; [102–104]) and practically [100, 105–107]. Such issues become critical for examining models such as Lévy Walk, where animal movement should be scale-independent (see [108] and references therein) and needs to be examined as such [85, 109]. Solutions require sampling animal position with higher temporal resolution [110–112], which may be possible for larger animals [86, 109] with improvements in GPS technology [113] but, ultimately, fixes need to resolve the minimum radius tortuosity [100].

The GPS-enabled dead-reckoning method described in the current study is the only method by which distance and animal tortuosity can be measured accurately

independent of any bias due to scale [31, 38]. Not only should this method provide new information on the habits of animals, but it offers a means for acquiring data on, and testing recent theoretical developments in movement ecology such as Correlated Random Walks, Levy Flights and State-space models (c.f. [114–122]). Given that tortuosity and movement patterns are likely to vary between species, populations and individuals, this new tool available to animal ecologists may be the only means to measure this variation properly, and should be considered a significant development in the understanding of movement ecology [100, 123].

Conclusions

Dead-reckoning has the potential to record the fine scale movement of terrestrial animals. To obtain the same level of detail from GPS telemetry alone, devices would require large amounts of power and could induce bias at small scales. Despite dead-reckoning having been employed on aquatic species, numerous methodological barriers restricted its use on terrestrial species. This study is the first explicit demonstration of terrestrial dead-reckoning and should provide adequate information to be used by those researchers of terrestrial species that are currently limited to temporally sparse GPS telemetry. These continuous, fine scale dead-reckoned tracks should record animal movement on a step by step basis, providing a complete account of animal location and movement. Initially, estimation of speed for integration in dead-reckoning calculations was problematic for terrestrial animals, but this issue has been largely overcome by use of accelerometers and a novel correction method that makes use of secondary ground truth positions. This technique has the potential to develop our understanding of animal movement ecology, and inform movement models that better reflect the true nature of animal movement patterns.

Availability of supporting data

A video detailing the dead reckoning validation experiment and illustration of results depending on different correction regimes is available in Additional File 1.

Additional file

Additional file 1: Video detailing dead reckoning validation experiment and illustration of results depending on different correction regimes. (MP4 14701 kb)

Competing interests

The authors have no competing interests to declare.

Authors' contributions

R.P.W. conceived of the study. O.R.B., J.S.W., M.W.J., M.D.H., and R.P.W. developed the methodology. O.R.B., J.S.W., M.W.J., M.D.H., D.M.S., N.J.M., E.A.M., I.E.M., and R.P.W. collected or analysed data. R.P.W. & O.R.B. drafted the

manuscript with assistance from J.S.W. and M.W.J. All authors read and approved the final manuscript.

Acknowledgements

OB was funded by a KESS PhD studentship and an Alexander von Humboldt Post-Doctoral Fellowship. JSW was funded by an EPSRC doctoral training grant. IEM and EAM were funded by PhD studentships from the Department of Employment and Learning (DEL) and the Department of Agriculture and Rural Development (DARD), Northern Ireland, respectively. Thanks go to Megan Woodhouse for her assistance in data collection on the horse.

Author details

¹Institut für Terrestrische und Aquatische Wildtierforschung, Stiftung Tierärztliche Hochschule, Hannover, Werfstr. 6, 25761 Büsum, Germany. ²Department of Computer Science, College of Science, Swansea University, Singleton Park, Swansea SA2 8PP, Wales, UK. ³College of Engineering, Swansea University, Singleton Park, Swansea SA2 8PP, Wales, UK. ⁴Faculté des Sciences de la Vie, Master d'Ecophysiologie et Ethologie, Université de Strasbourg, 28 rue Goethe, 67083 Strasbourg Cedex, France. ⁵School of Biological Sciences, Institute for Global Food Security, Queen's University Belfast, Belfast BT9 7BL Northern Ireland, UK. ⁶Swansea Lab for Animal Movement, Biosciences, College of Science, Swansea University, Singleton Park, Swansea SA2 8PP, Wales, UK.

Received: 21 January 2015 Accepted: 6 September 2015

Published online: 15 September 2015

References

- Stephens DW, Brown JS, Ydenberg RC. Foraging: behaviour and ecology. Chicago: Chicago University Press; 2007.
- Stephens DW, Krebs JR. Foraging theory. Princeton NJ: Princeton University Press; 1986.
- Swingland IR, Greenwood PJ. The ecology of animal movement. Oxford: Clarendon; 1983.
- Nathan R, Getz WM, Revilla E, Holyoak M, Kadmon R, Saltz D, et al. A movement ecology paradigm for unifying organismal movement research. *Proc Natl Acad Sci*. 2008;105(49):19052–9. doi:10.1073/pnas.0800375105.
- Dale VH, Brown S, Haeuber RA, Hobbs NT, Huntly N, Naiman RJ, et al. Ecological principles and guidelines for managing the use of land. *Ecol Appl*. 2000;10(3):639–70.
- Kot M, Lewis MA, van den Driessche P. Dispersal data and the spread of invading organisms. *Ecology*. 1996;77(7):2072–42.
- Stinner RE, Barfield CS, Stimac JL, Dohse L. Dispersal and movement of insect pests. *Annu Rev Entomol*. 1983;28:319–35.
- Patz JA, Daszak P, Tabor GM, Aquirre AA, Pearl M, Epstein J, et al. Unhealthy landscapes: Policy recommendations on land Use change and infectious disease emergence. *Environ Health Perspect*. 2004;112(10):1092–8.
- Davis L, Boersma P, Court G. Satellite telemetry of the winter migration of Adélie penguins *Pygoscelis adeliae*. *Polar Biol*. 1996;16(3):221–5. doi:10.1007/bf02329210.
- Roper TJ, Ostler JR, Schmid TK, Christian SF. Sett use in european badger *meles meles*. *Behaviour*. 2001;138(2):173–87.
- Cooke SJ, Hinch SG, Wikelski M, Andrews RD, Kuchel LJ, Wolcott TG, et al. Biotelemetry: a mechanistic approach to ecology. *Trends Ecol Evol*. 2004;19(6):334–43.
- White GC, Garrott RA. Analysis of wildlife radiotracking data. 1990.
- Rodgers AR. Tracking animals with GPS: the first ten years. In: Sibbald AM, Gordon IL, editors. *Tracking animals with GPS*. Aberdeen, Scotland: The Macaulay Institute; 2001.
- Recio MR, Mathieu R, Maloney R, Seddon PJ. Cost comparison between GPS and VHF based telemetry: case study of feral cats *Felis catus* in New Zealand. *N Z J Ecol*. 2011;35(1):114–7.
- Fancy SG, Pank LF, Douglas DC, Curby CH, Gerner GW, Amstrup SC, et al. Satellite telemetry: a new tool for wildlife research and management. *United States Fish and Wildlife Service Research Publications*. 1988;172:1–54.
- Hulbert IAR, French J. The accuracy of GPS for wildlife telemetry and habitat mapping. *J Appl Ecol*. 2001;38:869–78.
- Frair JL, Nielsen SE, Merrill EH, Lele SR, Boyce MS, Munro RHM, et al. Removing GPS collar bias in habitat selection studies. *J Appl Ecol*. 2004;41(2):201–12.
- Dussault C, Courtois R, Ouellet J, Huot J. Evaluation of GPS telemetry collar performance for habitat studies in the boreal forest. *Wildl Soc Bull*. 1999;27(4):965–72.
- Gamo RS, Rumble MA, Lindzey F, Stefanich M. GPS radio collar 3D performance as influenced by forest structure and topography. *Biotelemetry*. 2000;15:464–73.
- D'Eon RG, Serrouya GS, Kochanny CO. GPS radiotelemetry error and bias in mountainous terrain. *Wildl Soc Bull*. 2002;30(2):430–9.
- Guillemette M, Woakes A, Flagstad A, Butler PJ. Effects of data-loggers implanted for a full year in female common Eiders. *Condor*. 2002;104:448–52.
- Reynolds DR, Riley JR. Remote-sensing, telemetric and computer-based technologies for investigating insect movement: a survey of existing and potential techniques. *Comput Electron Agric*. 2002;35:271–307.
- Bridger CJ, Booth RK. The effects of biotelemetry transmitter presence and attachment procedures on fish physiology and behaviour. *Rev Fish Sci*. 2003;11:13–34.
- Zavalaga CB, Halls JN, Mori GP, Taylor SA, Dell'Omo G. At-sea movement patterns and diving behaviour of Peruvian boobies *Sula variegata* in northern Peru. *Mar Ecol Prog Ser*. 2010;404:259–74.
- Witte TH, Wilson AM. Accuracy of non-differential GPS for the determination of speed over ground. *J Biomech*. 2004;37:1891–8.
- Kramer DL, McLaughlin RL. The behavioural ecology of intermittent locomotion. *Am Zool*. 2001;41:137–53.
- Morales JM, Moorcroft PR, Matthiopoulos J, Frair JL, Kie JG, Powell RA, et al. Building the bridge between animal movement and population dynamics. *Philosophical Transactions of the Royal Society, Biological Sciences*. 2010;365(1550):2289.
- Bramanti M, Dall'antonia L, Papi F. A new technique to follow the flight paths of birds. *J Exp Biol*. 1988;134:467–72.
- Wilson RP, Wilson MP. Dead reckoning- a new technique for determining penguin movements at sea. *Meeresforschung- Reports on Marine Research*. 1988;32:155–8.
- Wilson RP, Wilson MP, Link R, Mempel H, Adams NJ. Determination of movements of African penguins *spheniscus demersus* using a compass system - dead reckoning may be an alternative to telemetry. *J Exp Biol*. 1991;157:557–64.
- Wilson RP, Liebsch N, Davies IM, Quintana F, Weimerskirch H, Storch S, et al. All at sea with animal tracks; methodological and analytical solutions for the resolution of movement. *Deep-Sea Res II*. 2007;54:193–210.
- Wilson RP. Movements in Adélie penguins foraging for chicks at Ardley Island, Antarctica; circles within spirals, wheels within wheels. *Polar Biol*. 2002;15:75–87.
- Shiomi K, Sato K, Mitamura H, Arai N, Naito Y, Ponganis PJ. Effect of ocean current on the dead-reckoning estimation of 3-D dive paths of emperor penguins. *Aquat Biol*. 2008;3:265–70.
- Johnson MP, Tyack PL. A digital acoustic recording tag for measuring the response of wild marine mammals to sound. *IEEE J Ocean Eng*. 2003;28:3–12.
- Mitani Y, Sato K, Ito S, Cameron MF, Siniff DB, Naito Y. A method for reconstructing three-dimensional dive profiles of marine mammals using geomagnetic intensity data: results from two lactating Weddell seals. *Polar Biol*. 2003;26:311–7.
- Sims DW, Southall EJ, Tarling GA, Metcalfe JD. Habitat-specific normal and reverse diel vertical migration in the plankton-feeding basking shark. *J Anim Ecol*. 2005;74:755–61.
- Bradshaw CJA, Hindell MA, Sumner MD, Michael K. Loyalty pays: potential life history consequences of fidelity to marine foraging regions by southern elephant seals. *Anim Behav*. 2004;68:1349–60.
- Wilson RP, Shepard ELC, Liebsch N. Prying into the intimate details of animal lives: use of a daily diary on animals. *Endanger Species Res*. 2008;4:123–37.
- Ware C, Friedlaender AS, Nowacek DP. Shallow and deep lunge feeding of humpback whales in fjords of the West Antarctic Peninsula. *Mar Mamm Sci*. 2011;27(3):587–605.
- Davis RW, Fuiman LA, Williams TM, Le Boeuf BJ. Three-dimensional movements and swimming activity of a northern elephant seal. *Comp Biochem Physiol A*. 2001;129:759–70.
- Shepard ELC, Wilson RP, Quintana F, Gómez Laich A, Forman DW. Pushed for time or saving on fuel: fine-scale energy budgets shed light on currencies in a diving bird. *Proc R Soc B Biol Sci*. 2009;276(1670):3149–55. doi:10.1098/rspb.2009.0683.

42. Yoda K, Naito Y, Sato K, Takahashi A, Nishikawa J, Ropert-Coudert Y, et al. A new technique for monitoring the behaviour of free-ranging Adelie penguins. *J Exp Biol.* 2001;204:685–90.
43. Yoda K, Sato K, Niizuma Y, Kurita M, Bost CA, Le Maho Y, et al. Precise monitoring of porpoising behaviour of Adelie penguins determined using acceleration data loggers. *J Exp Biol.* 1999;202:3121–6.
44. Sato K, Mitani Y, Cameron MF, Siniff DB, Naito Y. Factors affecting stroking patterns and body angle in diving Weddell seals under natural conditions. *J Exp Biol.* 2003;206:1461–70.
45. Ropert-Coudert Y, Grémillet D, Kato A. Swim speeds of free-ranging great cormorants. *Mar Biol.* 2006;149:415–22.
46. Eckert SA. Swim speed and movement patterns of gravid leatherback sea turtles (*Dermochelys coriacea*) at St Croix, US Virgin Islands. *J Exp Biol.* 2002;205:3689–97.
47. Hassrick JL, Crocker DE, Zeno RL, Blackwell SB, Costa DP, Le Boeuf BJ. Swimming speed and foraging strategies of northern elephant seals. *Deep-Sea Res II.* 2007;54:369–83.
48. Ponganis PJ, Ponganis EP, Ponganis KV, Kooyman GL, Gentry RL, Trillmich F. Swimming velocities in otariids. *Can J Zool.* 1990;68:2105–12.
49. Wilson RP, Pütz K, Bost CA, Culik BM, Bannasch R, Reins T, et al. Diel dive depth in penguins in relation to diel vertical migration of prey: whose dinner by candle-light? *Mar Ecol Prog Ser.* 1993;94:101–4.
50. Shepard ELC, Wilson RP, Liebsch N, Quintana F, Laich AG, Lucke K. Flexible paddle sheds new light on speed: a novel method for the remote measurement of swim speed in aquatic animals. *Endanger Species Res.* 2008;4:157–64.
51. Dall'Antonia L, Dall'Antonia P, Benvenuti S, Ioale P, Massa B, Banadonna F. The homing behaviour of Cory's shearwaters (*Calonectris diomedea*) studied by means of a direction recorder. *J Exp Biol.* 1995;198:359–62.
52. Bidder OR, Soresina M, Shepard ELC, Halsey LG, Quintana F, Gomez Laich A, et al. The need for speed: testing overall dynamic body acceleration for informing animal travel rates in terrestrial dead-reckoning. *Zoology.* 2012;115:58–64.
53. Bidder OR, Qasem LA, Wilson RP. On Higher Ground: How Well Can Dynamic Body Acceleration Dertermine Speed in Variable Terrain? *PLoS One.* 2012; doi:10.1371/journal.pone.0050556.
54. Campbell HA, Gao L, Bidder OR, Hunter J, Franklin CE. Creating a behavioural classification module for acceleration data: using a captive surrogate for difficult to observe species. *J Exp Biol.* 2013;216:4501–6.
55. Brown DD, Kays R, Wikelski M, Wilson RP, Klimley AP. Observing the unwatchable through acceleration logging of animal behavior. *Anim Biotechnol.* 2013;1:20.
56. Shepard ELC, Wilson RP, Albareda D, Glesis A, Laich AG, Halsey LG, et al. Identification of animal movement patterns using tri-axial accelerometry. *Endanger Species Res.* 2008;10:47–60.
57. Shepard ELC, Wilson RP, Halsey LG, Quintana F, Gomez Laich A, Gleiss AC, et al. Derivation of body motion via appropriate smoothing of acceleration data. *Aquat Biol.* 2008;4:235–41.
58. Tanaka H, Takagi Y, Naito Y. Swimming speeds and buoyancy compensation of migrating adult chum salmon *Oncorhynchus keta* revealed by speed/depth/acceleration data logger. *J Exp Biol.* 2001;204:2895–3904.
59. Fang L, Antsaklis PJ, Montestruque LA, McMickell MB, Lemmon M, Sun Y et al. Design of a wireless assisted pedestrian dead reckoning system - the NavMote experience. *IEEE Transactions on Instrumentation and Measurement* .2005. p. 2342–58.
60. Qasem LA, Cardew A, Wilson A, Griffiths IW, Halsey LG, Shepard ELC, et al. Tri-Axial Dynamic Acceleration as a Proxy for Animal Energy Expenditure; Should we be summing or calculating the vector? *PLoS One.* 2012;7(2):e31187.
61. Fourati H, Manamanni N, Afilal L, Handrich Y. Posture and body acceleration tracking by inertial and magnetic sensing: Application in behavioral analysis of free-ranging animals. *Biomed Signal Process Control.* 2011;6(1):94–104.
62. Noda T, Okuyama J, Koizumi T, Arai N, Kobayashi M. Monitoring attitude and dynamic acceleration of free-moving aquatic animals using a gyroscope. *Aquat Biol.* 2012;16:265–75.
63. Noda T, Kawabata Y, Arai N, Mitamura H, Watanabe S. Monitoring escape and feeding behaviours of a cruiser fish by inertial and magnetic sensors. *PLoS One.* 2013;8(11):e79392. doi:10.1371/journal.pone.0079392.
64. Noda T, Kawabata Y, Arai N, Mitamura H, Watanabe S. Animal-mounted gyroscope/accelerometer/magnetometer: In situ measurement of the movement performance of fast-start behaviour in fish. *J Exp Mar Biol Ecol.* 2013;451:55–68.
65. Park K, Chung D, Chung H, Lee JG. Dead reckoning navigation of a mobile robot using an indirect Kalman filter. Washington, D. C: IEEE/SICE/RSJ International Conference on Multisensor Fusion and Integration for Intelligent Systems; 1996. p. 132–8.
66. Jimenez AR, Seco F, Prieto C, Guevara J. A comparison of pedestrian dead-reckoning algorithms using a low-cost MEMS IMU. Budapest, Hungary: IEEE International Symposium on Intelligent Signal Processing; 2009.
67. Randell C, Djalllis C, Muller H. Personal position measurement using dead reckoning. New York, USA: Seventh IEEE International Symposium on Wearable Computers; 2003. p. 166.
68. Caruso MJ. Applications of magnetic sensors for low cost compass systems. Position Location and Navigation Symposium, IEEE. San Diego, CA, USA: Honeywell, SSEC; 2000. p. 177–84.
69. Shiomi K, Narazaki T, Sato K, Shimatani K, Arai N, Ponganis PJ, et al. Data-processing artefacts in three-dimensional dive path reconstruction from geomagnetic and acceleration data. *Aquat Biol.* 2010;8:299–304.
70. Watanuki Y, Niizuma Y, Gabrielsen GW, Sato K, Naito Y. Stroke and glide of wing-propelled divers: deep diving seabirds adjust surge frequency to buoyancy change with depth. *Proc R Soc.* 2003;270:483–8.
71. Watanuki Y, Takahashi A, Daunt F, Wanless S, Harris M, Sato K, et al. Regulation of stroke and glide in a foot-propelled avian diver. *J Exp Biol.* 2005;208:2207–16.
72. Denne W. Magnetic compass deviation and correction. 3rd ed. Dobbs Ferry, NY: Sheridan House; 1979.
73. Caruso MJ. Application of magnetoresistive sensors in navigation systems, SAE Transaction, 1997. vol. 106, pp.1092–1098.
74. Skvortzov VY, Lee H, Bang S, Lee Y. Application of Electronic Compass for Mobile Robot in an Indoor Environment. Roma, Italy: IEEE International Conference on Robotics and Automation; 2007. p. 2963–70.
75. Hoff B, Azuma R. Autocalibration of an Electronic Compass in an Outdoor Augmented Reality System. Munich, Germany: Proceedings of IEEE and ACM International Symposium on Augmented Reality; 2000. p. 159–64.
76. Van Bergeijk J, Goense D, Keesman KJ, Speelman L. Digital filters to integrate global positioning system and dead reckoning. *J Agric Eng Res.* 1998;70:135–43.
77. Vasconcelos JF, Elkaim G, Silvestre C, Oliveira P. Geometric approach to strapdown magnetometer calibration in sensor frame. *IEEE Trans Aerosp Electron Syst.* 2011;47:1293–306.
78. Renaudin V, Afzal MH, Lachapelle G. Complete triaxis magnetometer calibration in the magnetic domain. *Hindawi Journal of Sensors.* 2010; doi:10.1155/2010/967245.
79. Dong W, Lim KY, Goh YK, Nguyen KD, Chen I, Yeo SH, et al. A low-cost motion tracker and its error analysis. Pasadena, CA: IEEE International Conference on Robotics and Automation; 2008. p. 311–6.
80. Guo P, Qiu H, Yang Y, Ren Z. The soft iron and hard iron calibration method using extended kalman filter for attitude and heading reference system. Position, Location and Navigation Symposium, 2008. Monterey, CA: IEEE/ION; 2008. p. 1167–74.
81. Gebre-Egziabher D, Elkaim GH, Powell JD, Parkinson BW, editors. A non-linear, two step estimation algorithm for calibrating solid-state strapdown magnetometers, Proceedings of the 8th International Conference on Integrated Navigation Systems. 2001.
82. Xiang H, Tian L. Development of a low-cost agricultural remote sensing system based on an autonomous unmanned aerial vehicle (UAV). *Biosyst Eng.* 2011;108:174–90.
83. Merkl J, Säll J. Indoor Navigation Using Accelerometer and Magnetometer. Linköpings Universitet: Linköpings Universitet; 2011.
84. Kwanmuang L, Ojeda L, Borenstein J. Magnetometer-enganced personal locator for tunnels and gps-denied outdoor environments. Proceedings of the SPIE Defense, Security and Sensing; Unmanned Systems Technology XIII; Conference DS117: Unmanned, Robotic and Layered Systems, Orlando, April 25–29, 2011.
85. Frair JL, Fieberg J, Hebblewhite M, Cagnacci DN, Pedrotti L. Resolving issues of imprecise and habitat-biased locations in ecological analyses using GPS telemetry data. *Philosophical Transactions of the Royal Society, Biological Sciences.* 2010;365:2187–200.
86. Ganskopp DC, Johnson DD. GPS error in studies addressing animal movements and activities. *Rangel Ecol Manag.* 2007;60:350–8.
87. Grémillet D, Dell'Omo G, Ryan PG, Peters G, Ropert-Coudert Y, Weeks SJ. Offshore diplomacy, or how seabirds mitigate intra-specific competition: a case study based on GPS tracking of Cape gannets from neighbouring colonies. *Mar Ecol Prog Ser.* 2004;268:265–79.

88. Schofield G, Bishop MA, MacLean G, Brown P, Baker M, Katselidis KA, et al. Novel GPS tracking of sea turtles as a tool for conservation management. *J Exp Mar Biol Ecol.* 2007;347:58–68.
89. Weimerskirch H, Bonadonna F, Bailleul F, Mabile G, Dell'Omo G, Lipp HP. GPS tracking of foraging albatrosses. *Science.* 2002;295:1259.
90. Garcia-Ripolles C, Lopez-Lopez P, Urios V. First description of migration and winterinf of adlt Egyptian vultures *Neophron percnopterus* tracked by GPS satellite telemetry. *Bird Study.* 2010;57:261–5.
91. Nelson ME, Mech LD, Frame PF. Tracking of white-tailed deer migration by global positioning system. *J Mammal.* 2004;85:505–10.
92. de Beer Y, Kilian W, Versfeld W, van Aarde RJ. Elephants and low rainfall alter woody vegetation in Etosha National Park Namibia. *J Arid Environ.* 2006;64:412–21.
93. Tomkiewicz SM, Fuller MR, Kie JG, Bates KK. Global positioning system and associated technologies in animal behaviour and ecological research. *Proc R Soc.* 2010;365:2163–76.
94. Moen R, Pastor J, Cohen Y, Schwartz CC. Effects of moose movement and habitat use on GPS collar performance. *J Wildl Manag.* 1996;60:659–68.
95. Cargnelli B, Coulon A, Hewison AJM, Goulard M, Angibault JM, Morellet N. Testing global positioning system performance for wildlife monitoring using mobile collars and known reference points. *J Wildl Manag.* 2007;71:1380–7.
96. Sager-Fradkin KA, Jenkins KJ, Hoffman RA, Happe PJ, Beecham JJ, Wright RG. Fix success and accuracy of global positioning system collars in old-growth temperate coniferous forests. *J Wildl Manag.* 2007;71:1298–308.
97. Heard DC, Ciarniello LM, Seip DR. Grizzly bear behavior and global positioning system collar fix rates. *J Wildl Manag.* 2008;72:596–602.
98. Hebblewhite M, Percy M, Merrill EH. Are all global positioning system collars created equal? Correcting habitat-induced bias using three brands in the Central Canadian Rockies. *J Wildl Manag.* 2007;71:2026–33.
99. Walker JS, Jones MW, Laramie RS, Holton MD, Shepard ELC, Williams HJ et al. Prying into the intimate secrets of animal lives; software beyond hardware for comprehensive annotation in 'Daily Diary' tags. submitted to *Movement Ecology.* in review.
100. Rowcliffe JM, Carbone C, Kays R, Branstaurer B, Jansen PA. Bias in estimating animal travel distance: the effect of sampling frequency. *Methods Ecol Evol.* 2012;3:653–62.
101. Whittington J, St. Clair CC, Mercer G. Path tortuosity and the permeability of roads and trails to wolf movement. *Ecology and Society.* 2004;9(1):4.
102. Bovet P, Benhamou S. Spatial analysis of animals' movements using a correlated random walk model. *J Theor Biol.* 1988;131:419–33.
103. Benhamou S. How to reliably estimate the tortuosity of an animal's path: straightness, sinuosity, or fractal dimension? *J Theor Biol.* 2004;229(2):209–20. doi:10.1016/j.jtbi.2004.03.016.
104. Codling EA, Hill NA. Sampling rate effects on measurement of correlated and biased random walks. *J Theor Biol.* 2005;233:573–88.
105. Zalewski A, Jedrzejewski W, Jedrzejewski B. Pine martens home ranges, numbers and predation on vertebrates in a deciduous forest Bialowieza National Park. Poland *Annales Zoologici Fennici.* 1995;32:131–44.
106. Musiani M, Okarma H, Jedrzejewski. Speed and actual distances travelled by radiocollared wolves in Bialowieza Primeval Forest (Poland). *Acta Theriol.* 1998;43:409–16.
107. Safi K, Kranstauber B, Weinzierl R, Griffin L, Rees EC, Cabot D, et al. Flying with the wind: scale dependency of speed and direction measurements in modelling wind support in avian flight. *Mov Ecol.* 2013;1:4.
108. Viswanathan GM, da Luz MGE, Raposo EP, Stanley HE. The physics of foraging: An introduction to random searches and biological encounters. Cambridge: Cambridge University Press; 2011.
109. Hurford A. GPS measurement error gives rise to spurious 180 turning angles and strong directional biases in animal movement data. *PLoS One.* 2009;4:e5632.
110. Mills KJ, Patterson BR, Murray DL. Effects of variable sampling frequencies on GPS transmitter efficiency and estimated wolf home range size and movement distance. *Wildl Soc Bull.* 2006;34:1463–9.
111. Johnson DD, Ganskopp DC. GPS collar sampling frequency: Effects on measures of resource use. *Rangel Ecol Manag.* 2008;61:226–31.
112. Loneragan M, Fedak M, McConnell B. The effects of interpolation error and location quality on animal track reconstruction. *Mar Mamm Sci.* 2009;25:275–82.
113. Hebblewhite M, Haydon DT. Distinguishing technology from biology: a critical review of the use of GPS telemetry data in ecology. *Philosophical Transactions of the Royal Society, Biological Sciences.* 2010;365:2303–12.
114. Atkinson RPD, Rhodes CJ, Macdonald DW, Anderson RM. Scale-free dynamics in the movement patterns of jackals. *Oikos.* 2002;98(1):134–40. doi:10.1034/j.1600-0706.2002.980114.x.
115. Fritz H, Said S, Weimerskirch H. Scale-dependent hierarchical adjustments of movement patterns in a long-range foraging seabird. *Proc R Soc Lond Ser B.* 2003;270(1520):1143–8. doi:10.1098/rspb.2003.2350.
116. Weimerskirch H, Pinaud D, Pawlowski F, Bost C. Does prey capture induce area-restricted search? A fine-scale study using GPS in a marine predator, the Wandering albatross. *Am Nat.* 2007;170:734–43.
117. Mårell A, Ball JP, Hofgaard A. Foraging and movement paths of female reindeer: insights from fractal analysis, correlated random walks, and Lévy flights. *Can J Zool.* 2002;80(5):854–65. doi:10.1139/z02-061.
118. Ramos-Fernández G, Mateos JL, Miramontes O, Coch G. Lévy walk patterns in the foraging movements of spider monkeys (*Ateles geoffroyi*). *Behav Ecol Sociobiol.* 2004;55:223–30.
119. Viswanathan GM, Afanasyev V, Buldyrev SV, Murphy EJ, Prince PA, Stanley HE. Lévy flight search patterns of wandering albatrosses. *Nature.* 1996;381(6581):413–5.
120. Sims DW, Southall EJ, Humphries NE, Hays GC, Bradshaw CJA, Pitchford JW, et al. Scaling laws of marine predator search behaviour. *Nature.* 2008;451:1098–102.
121. Patterson TA, Thomas L, Wilcox C, Ovaskainen O, Matthiopoulos J. State-space models of individual animal movement. *Trends Ecol Evol.* 2008;23(2):87–94.
122. Reynolds AM, Rhodes CJ. The Lévy flight paradigm: Random search patterns and mechanisms. *Ecology.* 2009;90:877–87.
123. Holyoak M, Casagrandi R, Nathan R, Revilla E, Spiegel O. Trends and missing parts in the study of movement ecology. *Proc Natl Acad Sci.* 2008;105(49):19060–5. doi:10.1073/pnas.0800483105.

Submit your next manuscript to BioMed Central and take full advantage of:

- Convenient online submission
- Thorough peer review
- No space constraints or color figure charges
- Immediate publication on acceptance
- Inclusion in PubMed, CAS, Scopus and Google Scholar
- Research which is freely available for redistribution

Submit your manuscript at
www.biomedcentral.com/submit

